1 **Title**
2
3 NeuroTri2-VISDOT: An open-access tool to harness the power of second trimester human single cell data

4 to inform models of Mendelian neurodevelopmental disorders

5

6 **Authors**

7 Kelly J. Clark[1,2]*, Emily E. Lubin[1,2]*, Elizabeth M. Gonzalez[1,2], Annabel K. Sangree[1,2], Dana E. Layo-

8 Carris[2], Emily L. Durham[2], Rebecca C. Ahrens-Nicklas[2,3], Tomoki T. Nomakuchi[2+], Elizabeth J. Bhoj[2,3+]

9

10 **Author Affiliations**

11 [1] Biomedical Graduate School, University of Pennsylvania, Perelman School of Medicine

12 [2] Children's Hospital of Philadelphia

13 [3] Department of Pediatrics, University of Pennsylvania, Perelman School of Medicine

14 * co-first authors

15 + co-corresponding senior authors

16 Tomoki Nomakuchi – nomakuchit@chop.edu

17 Elizabeth Bhoj – bhoje@chop.edu

18

19 **<u>Abstract</u>**

20 Whole exome and genome sequencing, coupled with refined bioinformatic pipelines, have enabled

21 improved diagnostic yields for individuals with Mendelian conditions and have led to the rapid

22 identification of novel syndromes. For many Mendelian neurodevelopmental disorders (NDDs), there is a

23 lack of pre-existing model systems for mechanistic work. Thus, it is critical for translational researchers

24 to have an accessible phenotype- and genotype-informed approach for model system selection. Single-cell

25 RNA sequencing data can be informative in such an approach, as it can indicate which cell types express

26 a gene of interest at the highest levels across time. For Mendelian NDDs, such data for the developing

27 human brain is especially useful. A valuable single-cell RNA sequencing dataset of the second trimester

1

28   developing human brain was produced by Bhaduri et al in 2021, but access to these data can be limited by

29   computing power and the learning curve of single-cell data analysis. To reduce these barriers for

30   translational research on Mendelian NDDs, we have built the web-based tool, Neurodevelopment in

31   Trimester 2 - VIsualization of Single cell Data Online Tool (NeuroTri2-VISDOT), for exploring this

32   single-cell dataset, and we have employed it in several different settings to demonstrate its utility for the

33   translational research community.

34

35   **<u>Intro</u>**

36   Mendelian neurodevelopmental disorders (NDDs) are single-gene conditions that impact the

37   development and function of the brain[1]. Forty percent of the more than 5,000 currently classified

38   Mendelian disorders involve the brain or nervous system[2], and over 1,500 genes have been implicated in

39   these conditions[3]. Collectively, an estimated 9-18% of children are impacted by NDDs globally[3], with

40   approximately 3% of children diagnosed with a Mendelian NDD[1]. Every year more precise diagnoses are

41   provided to families as about 300 new genes are identified as harboring causative variants underlying

42   Mendelian NDDs[4]. Often, these novel NDDs fall into the classification of ultra-rare, impacting fewer than

43   1 in 50,000 individuals around the world[5].

44   Putative disease candidate genes can be identified either through individual cases and small cohorts,

45   or through the leveraging of large-scale publicly available datasets, such as gnomAD and GTEx[6–8] (Figure

46   1A). Clinicians who provide care to these individuals can then connect with each other via resources like

47   GeneMatcher and Matchmaker Exchange[9–11]. Through this approach, teams of clinicians and researchers

48   can identify larger cohorts who share causative variants in the same genes and build more robust

49   phenotypic profiles to inform care. Model systems are often not readily available to interrogate the

50   pathogenic mechanism of these conditions and, even when they exist, these models can be financially

51   prohibitive to obtain and space-prohibitive to maintain. Further, clinically accessible tissue (CATs) from

52   affected individuals, like blood and skin, are useful for mechanistic studies but their availability is limited

53   by research participation, logistical barriers and cost[12] (Figure 1A). This lack of preexisting functional

54   work and limited access to CATs for targeted assays can be a barrier to providing prognostic information

55   to families.

56   Thus, it is imperative for translational geneticists to have access to a systematic, phenotype-informed,

57   genotype-first approach to select a model system. Human induced pluripotent stem cells (hiPSC) are

58   powerful models, but it can be challenging to determine the most appropriate terminal lineage

59   differentiation that recapitulates the pathogenesis of a particular ultra-rare Mendelian syndrome,

60   especially if little to no functional work has been published for a gene of interest. Further, while model

61   organisms like mice and zebrafish are incredibly powerful, especially for interrogating systemic effects of

62   variants, obtaining and maintaining colonies of these organisms can be cost and time prohibitive.

63   Additionally, there are fundamental differences in neurodevelopment between these organisms and

64   humans that must be considered. Nonetheless, targeted exploration of specific cell types using *in vivo*

65   systems can fill existing gaps in our current ability to differentiate hiPSCs to all the cell types that make

66   up the human brain.

67   With the explosion of large-scale sequencing projects, an overwhelming number of datasets have

68   been generated, and resources like the Chan Zuckerberg Initiative's CELLxGENE platform help make

69   these data more accessible[13]. Identifying the dataset that best aligns with a specific research question can

70   still be a challenge. To specifically bridge the computational chasm for translational research questions

71   motivated by individuals with ultra-rare Mendelian NDDs, we have built the tool Neurodevelopment in

72   Trimester 2 - VIsualization of Single cell Data Online Tool (NeuroTri2-VISDOT). NeuroTri2-VISDOT

73   references the powerful second trimester human fetal brain single-cell RNA-sequencing dataset generated

74   by Bhaduri et al[14], which is an important dataset for many reasons. First, these data cannot be widely

75   generated, as access to fetal human brain tissue samples is limited. Additionally, generating and utilizing

76   single cell RNA-sequencing data is a complex and computationally demanding process. The teams who

77   produced these data have already overcome these two significant barriers to access. We sought to make

78   these data more accessible so that the field of translational genetics can use them to responsibly inform

79   selection of models of neurodevelopment, even without a robust computational background.

80   These second trimester data are an incredibly powerful window into human neurodevelopment

81   (Figure 1B). The development of the human central nervous system (CNS) begins after gestational week

82   3 (GW3), following the closure of the neural tube, a process called neurulation (Figure 1B)[15]. During the

83   first trimester, neural immune cells like native cells and microglia colonize the CNS and begin to

84   proliferate prior to the formation of the blood brain barrier[16–19] (Figure 1B, Table 1). Neurogenesis and

85   gliogenesis also begin in the first trimester but, at this stage, a limited number of cell types are identifiable

86   based on transcriptomic profiling, including radial glia (RG), neural progenitor cells (NPCs), and

87   neurons[20]. That stands in contrast to what can be delineated in the second trimester, where transient

88   prenatal cell types, such as Cajal-Retzius cells, as well as many of the CNS cell populations that persist

89   into post-natal life are captured (Figure 1B, gold box; Table 1). Processes essential to neurodevelopment

90   also occur during the second trimester. For instance, RG undergo the human-specific process of becoming

91   a physically discontinuous scaffold between GW16.5-17, which is not captured in commonly employed

92   model systems of neurodevelopment, such as mice or zebrafish[21,22].

93   There are thousands of unique cell types in the human brain. However, identifying all such cell types

94   using single-cell transcriptomic data remains a difficult task. Single cell RNA-sequencing has a high

95   degree of uncertainty, likely due to sequence-specific RNA degradation and random sampling of lowly

96   expressed genes. This results in many expression values being "zero"[23]. Further, identification of cell

97   types relies on unsupervised clustering followed by time-consuming manual annotation[23]. Thus, rare cell

98   types may be lumped into other clusters, cell types with variable expression patterns may be

99   misidentified, and differentiating continuous cell types must be put into discrete categories. For example,

100   at some point NPCs become neurons. This is a continuous process, but a line must be drawn between the

101   cell types at a discrete point. Cell atlases detailing the expression profiles of different tissues and cell

102   types will be a key resource for this part of single cell data analysis for all model organisms, but they are

103   still a work in progress for human cell types.

104   The dataset harnessed in NeuroTri2-VISDOT profiles 10 brain structures and 6 neocortical areas.

105   These data are resolved to 10 unique cell types by clustering each sample by cell type and sub-clustering

4

106   to identify more granular cell types[14]. We provide a primer on those cell populations to facilitate

107   interpretation of the visualized data using NeuroTri2-VISDOT (Table 1), but these cells have been

108   reviewed in more detail elsewhere[16–19,21,22,24–35,36]. We provide NeuroTri2-VISDOT as a free web-based

109   interface (https://kellyclark.shinyapps.io/NeuroTri2-VISDOT/) and as an open-access R Shiny application

110   via GitHub (https://github.com/kellyclark1/VISDOT) to visualize the expression patterns of genes across

111   cell types throughout the second trimester in the developing human brain.

112   In this paper, we employ NeuroTri2-VISDOT in several different settings to evaluate its utility for the

113   translational research community that focuses on Mendelian NDDs. First, we interrogate the expression

114   patterns of the causative genes linked to the subset of chromatinopathies associated with Rubinstein-

115   Taybi Syndrome (RSTS) (OMIM #613684; 180849). We then apply NeuroTri2-VISDOT to the spectrum

116   of syndromes categorized as Noonan Syndrome-like RASopathies, including Noonan Syndrome (NS)

117   (OMIM #163950; #610733; #616559; #613224; #616564; #605275; #619745; #615355; #618624;

118   #618499; #611553); NS with multiple lentigines (OMIM #151100); NS-like disorder with loose anagen

119   hair (OMIM #607721, 617506); Cardiofaciocutaneous Syndrome (OMIM #115150, 615279, 615280);

120   Costello Syndrome (OMIM #218040); CBL-related RASopathy (OMIM #613563); wide spectrum

121   RASopathy (OMIM #615278, 609942); MAPK1-related RASopathy (OMIM # 619087); and newly

122   described NS-like RASopathies caused by variants in CDC42 and YWHAZ[37,38]. Finally, we employ

123   NeuroTri2-VISDOT to an emerging class of NDDs caused by germline variants in histone genes[6,39].

124   Using NeuroTri2-VISDOT, we demonstrate that single cell RNA sequencing data from the developing

125   human brain can be used to motivate the evidence-based selection of relevant cell populations to explore

126   the pathogenic mechanism underlying Mendelian NDDs. Additionally, we show how systematic

127   visualization of the temporal gene expression profiles with NeuroTri2-VISDOT may help elucidate the

128   neurobiology underlying the neuro-phenotypic heterogeneity of historically grouped Mendelian NDDs.

129

Results

Using NeuroTri2-VISDOT

The NeuroTri2-VISDOT web-based interface has been designed to maximize the utility of the Bhaduri et al dataset for translational researchers (Supplemental Video 1). In the search box, an investigator can input the gene names for as many genes as they are interested in comparing using the notation from Ensembl GRCh38 Release 110 (Supplemental Figure 1A). Multiple genes must be space-separated, and gene names are case-sensitive. Users can opt to select or deselect any combination of cell types they are interested in exploring. All 10 cell types will always be represented in dot plots, but investigators may wish to deselect a cell type that has a higher expression than the other cell types for the line plots of percent and average expression. For example, the gene *PAFAH1B1 (LIS1)* is associated with the structural Mendelian NDD classical lissencephaly, a disorder primarily associated with cytoskeletal reorganization during neuron migration[40]. A large percent of second trimester Cajal-Retzius cells (~80%) express *PAFAH1B1* (Supplemental Figure 1B, top), which can obscure the percent of other cell types expressing the gene. By removing Cajal-Retzius cells from the line plots, an investigator could more closely interrogate the pattern of *PAFAH1B1* expression in the nine other cell types (Supplemental Figure 1B, bottom).

To enhance customizability, investigators can also specify the scale of the plots, which enables the standardization of axes across plots. The two scales that can be customized are those for average expression scaled and percent expression. Average expression scaled is the normalized expression values for that gene in that cell type, scaled to a mean of zero. Percent expression is the percentage of a particular cell type with at least one read mapping to the gene of interest[41]. Because genes can be expressed at a low level but still have large impacts on cell function and identity, we chose to focus on percent of cells expressing genes of interest rather than average expression of the gene in each cell in subsequent analyses but the ability to visualize both dimensions of expression is retained in NeuroTri2-VISDOT. Investigators are also able to download not only the individual plots but also the data visualized in the plots if they are interested in performing additional analyses.

6

Applying NeuroTri2-VISDOT to established NDD families

Chromatinopathies: A focus on Rubinstein-Taybi Syndrome (RSTS)

Chromatinopathies are caused by germline variants in genes that encode for epigenetic machinery: the readers, writers, erasers, and remodelers of the epigenome[42]. This group of Mendelian disorders is highly variable at both the genotypic and phenotypic level. Here, we focus on *CREBBP* and *EP300*, genes which encode histone acetyltransferases in which germline variants are causative for RSTS. Post-natal therapeutic intervention with histone deacetylase inhibitors rescues the markers of neurological dysfunction in mouse models of RSTS, emphasizing the value of more deeply understanding the pathogenesis of this disorder to better understand all chromatinopathies[42]. RSTS is a particularly elegant example of locus heterogeneity underlying phenotypic variability. Individuals who harbor variants in *EP300* tend to have less severe clinical features compared to those with *CREBBP* variants[43–45]. For example, intellectual disability is typically more severe in individuals with causative *CREBBP* variants, as is autism or autistic behaviors and epilepsy[43–46].

This phenotypic severity seems to correlate with the second trimester single cell expression signatures (Figure 2A). Both genes show a peak in expression at GW18 in endothelial cells, reaching a percent expression of about 35% (Figure 2A, right, unfilled boxes). Interestingly, *CREBBP* is expressed in ~48% of Cajal-Retzius cells while *EP300* is only expressed in about 27% of this cell type. This difference in percent expression, specifically in Cajal-Retzius cells, may contribute to the more severe neurological phenotypes of individuals with *CREBBP*-related RSTS compared to individuals with *EP300*-related RSTS. Notably, neuroimaging findings in individuals with RSTS include partial/total agenesis or hypodysgenesis of the corpus callosum, and straight gyrus hypoplasia have also been observed, though the genic contributions have been incompletely delineated[47]. The transcript patterns coupled with the neuroradiologic phenotypes suggest that taking a gene- and cell type-informed approach to interrogate the pathogenic mechanism underlying RSTS may be an appropriate choice to disentangle clinical heterogeneity.

182   *RASopathies: A focus on Noonan Syndrome and Noonan Syndrome-like (NS/NS-like) RASopathies*

183   RASopathies, like chromatinopathies, are a genotypically and phenotypically heterogenous group of

184   clinically overlapping Mendelian NDDs caused by variants affecting members and modulators of the

185   RAS-MAPK cascade. Here, we focus on NS and NS-like RASopathies because of their universal

186   classification as multisystem developmental disorders that often includes the CNS, which is not the case

187   for non-NS-like RASopathies[38]. The characteristic inclusion of a neurologic phenotype in NS and NS-like

188   RASopthies makes this variable group of syndromes amenable to interrogation with this

189   neurodevelopmental dataset.

190   In concordance with previously published work, we define NS-associated genes as *PTPN11, SOS1,*

191   *SOS2, NRAS, LZTR1, SPRED2, RIT1, RRAS2, MRAS* and *RAF1*[37,38] (Figure 2B, left). Of the NS-like

192   RASopathies, we define the associated genes as: *PTPN11* associated with NS with multiple lentigines;

193   *SHOC2* and *PPP1CB* associated with NS-like disorder with loose anagen hair*; BRAF, MAP2K1* and

194   *MAP2K2* associated with cardiofaciocutaneous syndrome; *HRAS* associated with Costello Syndrome; and

195   *CBL*, *KRAS*, *MAPK1*, *CDC42*, and YWHAZ associated with other RASopathies[37,38] (Figure 2B, right).

196   When we plot all NS/NS-like RASopathies together, it is challenging to identify any discernable patterns

197   (Supplemental Figure 2)**.** However, when we stratify based on the association of genes with NS compared

198   to NS-like RASopathies, trends begin to emerge (Figure 2C, 2D). Nine of the 10 NS genes could be

199   plotted (*RRAS2* was not able to be queried). Seven of these 9 genes have a peak at GW18 that transcends

200   cell type (Figure 2C, left, unfilled boxes). Additionally, these same genes exhibit an upward trend in

201   expression in both endothelial cells and Cajal-Retzius cells, which is consistent with what we observe

202   when looking at the percent expression line plots (Figure 2C, right, pink and green). Taken together, there

203   is a fairly consistent expression signature shared by genes that harbor causative variants in NS.

204   Compared to the NS genes, we observe heterogeneity in the second trimester brain expression of the

205   NS-like RASopathy genes (Figure 2D). The first observation is that both the dot plots and the line plots

206   for the newly described NS-like RASopathies associated with *CDC42* and *YWHAZ* do not follow the

207   same trends as other NS-like RASopathy causative genes (Figure 2D, unfilled arrows). In general, the

8

208   average and percent expression of these two genes throughout the second trimester is consistently greater

209   than what we observe for any other gene queried in this NS-like RASopathy analysis (Figure 2D). The

210   expression profiles visualized through the percent expression line plots is distinct in comparison to the

211   other NS/NS-like RASopathy genes (Figure 2D, right, unfilled arrows). It has been previously noted that

212   the assignment of the conditions caused by variants in these genes to the RASopathy family is under

213   debate[38]. These data, along with other disparate features of *CDC42* and *YWHAZ-* related disorders, may

214   support the reevaluation of the assignment of these conditions to the RASopathy family.

215   The value of looking at both the dot plots and the percent expression line plots is exemplified

216   when probing the genes that underly NS-like disorder with loose anagen hair: *SHOC2* and *PPP1CB*. The

217   dot plots for these genes look similar to each other, but distinct from other NS-like RASopathy genes

218   (Figure 2D, left). However, the percent expression plots of these genes in different cell types across the

219   second trimester are profoundly different. *SHOC2* has a bimodal peak in percent expression in Cajal-

220   Retzius cells at GW18 and GW20 (Figure 2D, right, gray arrows). Conversely, *PPP1CB* has a single peak

221   in percent expression at GW20 in Cajal-Retzius cells, as well as a peak in expression at GW16 in

222   forebrain RG cells. As with the case of *CREBBP* or *EP300*-derived RSTS, these data may support the use

223   of different model systems, for example Cajal-Retzius cells and/or forebrain RG, to study NS-like

224   disorder with loose anagen hair driven by causative variants in different genes. Investigating pathogenic

225   mechanisms through a bifurcated approach that centers on multiple cell types could enable the

226   identification of a shared, downstream perturbation that could be targeted through therapeutic

227   intervention.

228   Strikingly, the peak in expression at GW16 in forebrain RG cells that we observe in *PPP1CB-*

229   related NS-like disorder with loose anagen hair is also present in percent expression plots for *MAP2K2-*

230   related cardiofaciocutaneous syndrome, *HRAS*-related Costello Syndrome and *KRAS*-related wide

231   spectrum RASopathy (Figure 2D, right, black arrows). These bimodal peaks in expression transcend NS-

232   like RASopathy delineations; gene specification subgroups defined by the ClinGen RASopathy Expert

233   Panel, in which genes with similar function and/or structure have been grouped[48] (Supplemental Figure

234   3); and genes that share a gain-of-function disease mechanism (Supplemental Figure 4). Analysis of these

235   expression signatures may prove useful for geneticists when making classification decisions about

236   whether multiple syndromes should be grouped together in one family or into distinct entities.

237

238   **Applying NeuroTri2-VISDOT to an emerging class of NDDs**

239   Germline variants in genes encoding histones are an emerging class of Mendelian NDDs[39], which

240   have recently been classified by OMIM. HIST1H1E syndrome/Rahman Syndrome (OMIM #617537) is

241   caused by germline variants in the gene *HIST1H1E/H1-4* which encodes the histone H1 linker protein.

242   Bryant-Li-Bhoj Syndrome (OMIM #619721, #619720) is caused by germline variants in *H3-3A* and *H3-*

243   *3B*, the genes that encode histone H3.3. Tessadori-Bicknell-van Haaften NDD (OMIM #619758,

244   #619759, #619950, #619551) is caused by germline variants in the genes *H4C3*, *H4C11*, *H4C5*, and

245   *H4C9*, the genes that encode H4. Additional histone-encoding genes, including *MACROH2A1*, *H2AZ1*,

246   *MACROH2A2*, *H2AZ2*, *H2AX*, and *H1-0*, are predicted to be putative disease candidates[6].

247   The genes linked to HIST1H1E syndrome and Tessadori-Bicknell-van Haaften NDD are classified as

248   replication-coupled (RC) histones, which are associated with unique structural and functional features.

249   RC histone genes encode the only known cellular mRNA transcripts that are not poly-adenylated[6]. This

250   lack of a polyA tail on RC histone transcripts renders them undetectable in the most common type of

251   library preparation method used for RNA-sequencing. This means that in most publicly available datasets,

252   including the one employed here, we are unable to explore their expression. Nonetheless, we are able to

253   interrogate the expression of replication-independent (RI) histones that do have polyA tails. Based on

254   prior work, we can stratify these RI histones into known NDD-causing, predicted NDD-causing, and non-

255   disease-causing groups[6] (Figure 3A).

256   When we plot the expression of these RI histones, all the genes known or predicted to be associated

257   with Mendelian NDDs show increases in expression across the second trimester, compared to genes not

258   known or predicted to be associated with NDDs, with the exception of *H1-10* (Figures 3B-D).

259   Additionally, these genes seem to have a peak in expression at GW16 irrespective of cell type (Figure 3B-

10

260   D, unfilled boxes). Interestingly, this is the window during which RG become physically

261   discontinuous[21,22]. This expression pattern suggests an importance for RI histones at this very early point

262   in brain development, and that RG would be an effective model to study the phenotypes associated with

263   these variants. Neuroimaging results from individuals with HIST1H1E Syndrome, Bryant-Li-Bhoj

264   Syndrome and Tessadori-Bicknell-van Haaften NDD do not show salient dysregulation of neural

265   migration or cortical development. Thus, the role of RG in the neuropathology of these syndromes has not

266   been explored. Through the visualization of these data using NeuroTri2-VISDOT, we identify a novel

267   terminal lineage to which hiPSCs can be differentiated for subsequent functional work. More broadly, this

268   demonstrates the utility of single cell expression signatures in development for identifying and supporting

269   NDD candidate genes.

270

271   **Discussion**

272   Clinical genetics is rooted in a rich history of clinical phenotyping that long predates the field's

273   ability to perform diagnostic genetic testing. In some cases, this has led to phenotypically similar

274   syndromes being grouped together under large umbrella characterizations, such as NDDs or

275   leukodystrophies, that may not reflect the distinct genetic processes contributing to the pathophysiology[1].

276   Now, the field of translational genetics is reckoning with this same question: to lump disorders together or

277   split them into functional groups[49]. With NeuroTri2-VISDOT, we introduce a tool that may prove a

278   valuable resource in this pursuit, with utility demonstrated for both established and emerging NDDs.

279   Single-cell RNA sequencing is an incredibly powerful method for exploring tissue heterogeneity and

280   gene expression across cell types. However, generating a single-cell dataset is expensive and availability

281   of human tissues, especially human fetal tissue, is limited. Further, data analysis requires computational

282   skills and high-performance computing due to the size and complexity of the multidimensional data

283   produced in these experiments. NeuroTri2-VISDOT seeks to address the computational barriers to use of

284   this valuable tool, particularly the size of single-cell data and the computational skills needed to explore

285   it. First, the complete dataset utilized here is available as a 50GB file, which is too large for many

11

286   researchers to store and use on their own computers necessitating the use of high-performance computing.

287   NeuroTri2-VISDOT stores a summary of this dataset online, with average scaled expression and percent

288   expression for each gene by cell type rather than read counts for each cell. No downloads are necessary to

289   use the web app, and the raw data for genes of interest can be downloaded as a small file of comma-

290   separated values, reducing the need to download the entire dataset. Second, analysis of single cell data

291   using the R package, Seurat, requires many researchers to dedicate significant time to learning how to

292   navigate R and Seurat objects. NeuroTri2-VISDOT reduces the need for coding expertise by allowing

293   exploration of single cell data with a user-friendly interface that requires only a gene or list of genes as

294   input.

295   We recognize some limitations associated with our approach. First, this dataset was generated from

296   single-cell transcriptomics performed on microdissected regions of the brain that included 10 major

297   forebrain, midbrain and hindbrain regions in addition to 6 neocortical areas, meaning that only cell types

298   identified in the neocortical samples were powered to be reported in the final dataset[14]. Thus, some

299   cellular populations important to neurodevelopment, such as cells of the cerebellum, are not represented.

300   Astrocytes, which differentiate from RG after the peak of neurogenesis at the end of the second trimester,

301   are also not represented. These cells play an important homeostatic role in the brain parenchyma and form

302   the neural component of the blood brain barrier. However, there are thousands of unique cell types in the

303   human brain, and it is not feasible to capture them all. Further, while these data provide a powerful

304   window into neurodevelopment by quantifying gene expression in the second trimester, earlier and later

305   stages of prenatal brain development are not captured here. Nonetheless, NeuroTri2-VISDOT is intended

306   not as an atlas of all cells in all stages of the developing brain, but rather as a tool to efficiently leverage

307   this powerful dataset in translational genetic research.

308   Another limitation of this analysis is the interdependence and interconnectivity of different cell types

309   during neurodevelopment. For instance, GABAergic interneurons and oligodendrocyte precursor cells

310   require the endothelial-lined vasculature to appropriately migrate. Additionally, NPCs not only arise from

311   but also migrate along RG before eventually differentiating into glutamatergic cortical neurons. This

312   complexity, in part, motivates some investigators to opt for model organisms, such as mice or zebrafish as

313   opposed to hiPSCs. The expression visualization made possible by NeuroTri2-VISDOT captures this

314   complexity, but also enables investigators to make evidence-based decisions about model selection. For

315   instance, if RG are nominated as a compelling model to interrogate, it is crucial to consider that this cell

316   type undergoes the process of becoming a physically discontinuous scaffold during the middle of the

317   second trimester, which may support the use of hiPSCs over mice and zebrafish in specific situations.

318   These data may also indicate that different cell populations are worth interrogating based on which gene

319   harbors variants driving the phenotype, as in the case of *CREBBP*- versus *EP300*-driven RSTS.

320   A biological consideration before employing these data is whether the RNA transcript is the

321   appropriate read out for a given gene of interest. Transcript and protein levels are discordant throughout

322   neurodevelopment, most prominently in post-natal life[50]. When exploring post-natal neurodevelopment,

323   protein or phosphorylated protein may be a more precise metric to inform model selection. In cases where

324   transcript level expression is an appropriate biologic read-out, such as in pre-natal neurodevelopment, we

325   propose that there are several ways in which NeuroTri2-VISDOT could be applied in the future (Figure

326   4). At the level of an individual translational research lab, we envision NeuroTri2-VISDOT as a tool to

327   enable investigators to systemically inform the selection of their model systems. We see this approach

328   being adapted by bioinformaticians to create similar tools for the increasingly available datasets designed

329   to ask similarly targeted questions. For example, a similar tool to visualize neural gene expression across

330   cell types across the lifespan could be employed by biobanks to identify and cluster gene expression

331   signatures of putative disease candidate genes.

332   In summary, the numerous applications of NeuroTri2-VISDOT, including model selection and

333   interrogation of gene signatures across time and cell types, allow for translational genetics researchers to

334   harness the power of a valuable single-cell second trimester brain dataset without requiring programming

335   experience or access to high performance computing resources. The approach employed to generate and

336   evaluate NeuroTri2-VISDOT also provides a framework for developing tools for similar datasets that will

337   be beneficial to the wider translational research community.

338   **Methods**

339   **Data extraction**

340   The Seurat object for the data generated by Bhaduri et al. is publicly available[14,41]. This object was

341   split into separate objects for each cell type, and plots were generated for genes of interest for each cell

342   type using the Seurat DotPlot function. The data in these dot plots were combined to create a large table

343   containing each gene with the percent expression and average expression scaled at each time point in each

344   cell type. This data is available to download from the NeuroTri2-VISDOT web app. Additionally, the

345   code used to generate NeuroTri2-VISDOT can be found at https://github.com/kellyclark1/VISDOT.

346

347   **NeuroTri2-VISDOT Web app development**

348   The NeuroTri2-VISDOT web app was written in R v4.2.2[51] using the R package shiny v1.7.3[52] and is

349   available at https://kellyclark.shinyapps.io/NeuroTri2-VISDOT/. Plots displayed on the web interface

350   were designed using ggplot2 v3.4.0[53].

351   The web app requires as input at least one human Ensembl GRCh38 Release 110 gene name and will

352   accept as many gene names as a user would like to compare. Users may also select cell types of interest

353   for line plots using the checkboxes in the left panel. The web app allows custom scaling for plots, which

354   should be used with caution. The intent of custom scaling is to allow multiple genes to be plotted

355   separately but at the same scale. However, setting limits that do not include the data will exclude data

356   points outside of those limits.

357

358 REFERENCES

359 1. Parenti I, Rabaneda LG, Schoen H, Novarino G. Neurodevelopmental Disorders: From Genetics to

360   Functional Pathways. *Trends in Neurosciences*. 2020;43(8):608-621. doi:10.1016/j.tins.2020.05.004

361 2. Rexach J, Lee H, Martinez-Agosto JA, Németh AH, Fogel BL. Clinical application of next-

362   generation sequencing to the practice of neurology. *The Lancet Neurology*. 2019;18(5):492-503.

363   doi:10.1016/S1474-4422(19)30033-X

364 3. Leblond CS, Le TL, Malesys S, et al. Operative list of genes associated with autism and

365   neurodevelopmental disorders based on database review. *Molecular and Cellular Neuroscience*.

366   2021;113:103623. doi:10.1016/j.mcn.2021.103623

367 4. Bamshad MJ, Nickerson DA, Chong JX. Mendelian Gene Discovery: Fast and Furious with No End

368   in Sight. *The American Journal of Human Genetics*. 2019;105(3):448-455.

369   doi:10.1016/j.ajhg.2019.07.011

370 5. Smith CIE, Bergman P, Hagey DW. Estimating the number of diseases – the concept of rare, ultra-

371   rare, and hyper-rare. *iScience*. 2022;25(8):104698. doi:10.1016/j.isci.2022.104698

372 6. Lubin E, Bryant L, Aicher J, Li D, Bhoj E. Analysis of histone variant constraint and tissue

373   expression suggests five potential novel human disease genes: H2AFY2, H2AFZ, H2AFY, H2AFV,

374   H1F0. *Hum Genet*. 2022;141(8):1409-1421. doi:10.1007/s00439-022-02432-1

375 7. Gudmundsson S, Singer-Berk M, Watts NA, et al. Variant interpretation using population databases:

376   Lessons from gnomAD. *Human Mutation*. 2022;43(8):1012-1030. doi:10.1002/humu.24309

377 8. Lonsdale J, Thomas J, Salvatore M, et al. The Genotype-Tissue Expression (GTEx) project. *Nat

378   Genet*. 2013;45(6):580-585. doi:10.1038/ng.2653

9. Sobreira N, Schiettecatte F, Valle D, Hamosh A. GeneMatcher: A Matching Tool for Connecting Investigators with an Interest in the Same Gene. *Human Mutation*. 2015;36(10):928-930. doi:10.1002/humu.22844

10. Hamosh A, Wohler E, Martin R, et al. The impact of GeneMatcher on international data sharing and collaboration. *Human Mutation*. Published online March 28, 2022:humu.24350. doi:10.1002/humu.24350

11. Azzariti DR, Hamosh A. Genomic Data Sharing for Novel Mendelian Disease Gene Discovery: The Matchmaker Exchange. *Annu Rev Genom Hum Genet*. 2020;21(1):305-326. doi:10.1146/annurev-genom-083118-014915

12. Aicher JK, Jewell P, Vaquero-Garcia J, Barash Y, Bhoj EJ. Mapping RNA splicing variations in clinically accessible and nonaccessible tissues to facilitate Mendelian disease diagnosis using RNA-seq. *Genetics in Medicine*. 2020;22(7):1181-1190. doi:10.1038/s41436-020-0780-y

13. CZI Single-Cell Biology Program, Abdulla S, Aevermann B, et al. *CZ CELL×GENE Discover: A Single-Cell Data Platform for Scalable Exploration, Analysis and Modeling of Aggregated Data*. Cell Biology; 2023. doi:10.1101/2023.10.30.563174

14. Bhaduri A, Sandoval-Espinosa C, Otero-Garcia M, et al. An atlas of cortical arealization identifies dynamic molecular signatures. *Nature*. 2021;598(7879):200-204. doi:10.1038/s41586-021-03910-8

15. Greene NDE, Copp AJ. Neural Tube Defects. *Annu Rev Neurosci*. 2014;37(1):221-242. doi:10.1146/annurev-neuro-062012-170354

16. Prinz M, Erny D, Hagemeyer N. Ontogeny and homeostasis of CNS myeloid cells. *Nat Immunol*. 2017;18(4):385-392. doi:10.1038/ni.3703

400 17. Herz J, Filiano AJ, Wiltbank AT, Yogev N, Kipnis J. Myeloid Cells in the Central Nervous System. *Immunity*. 2017;46(6):943-956. doi:10.1016/j.immuni.2017.06.007

402 18. McNamara NB, Munro DAD, Bestard-Cuche N, et al. Microglia regulate central nervous system myelin growth and integrity. *Nature*. 2023;613(7942):120-129. doi:10.1038/s41586-022-05534-y

404 19. Menassa DA, Gomez-Nicola D. Microglial Dynamics During Human Brain Development. *Front Immunol*. 2018;9:1014. doi:10.3389/fimmu.2018.01014

406 20. Eze UC, Bhaduri A, Haeussler M, Nowakowski TJ, Kriegstein AR. Single-cell atlas of early human brain development highlights heterogeneity of human neuroepithelial cells and early radial glia. *Nat Neurosci*. 2021;24(4):584-594. doi:10.1038/s41593-020-00794-1

409 21. Nowakowski TJ, Pollen AA, Sandoval-Espinosa C, Kriegstein AR. Transformation of the Radial Glia Scaffold Demarcates Two Stages of Human Cerebral Cortex Development. *Neuron*. 2016;91(6):1219-1227. doi:10.1016/j.neuron.2016.09.005

412 22. LaMonica BE, Lui JH, Wang X, Kriegstein AR. OSVZ progenitors in the human cortex: an updated perspective on neurodevelopmental disease. *Current Opinion in Neurobiology*. 2012;22(5):747-753. doi:10.1016/j.conb.2012.03.006

415 23. Lähnemann D, Köster J, Szczurek E, et al. Eleven grand challenges in single-cell data science. *Genome Biol*. 2020;21(1):31. doi:10.1186/s13059-020-1926-6

417 24. Daneman R, Prat A. The Blood–Brain Barrier. *Cold Spring Harb Perspect Biol*. 2015;7(1):a020412. doi:10.1101/cshperspect.a020412

419 25. Obermeier B, Daneman R, Ransohoff RM. Development, maintenance and disruption of the blood-brain barrier. *Nat Med*. 2013;19(12):1584-1596. doi:10.1038/nm.3407

421   26. Crouch EE, Bhaduri A, Andrews MG, et al. Ensembles of endothelial and mural cells promote

422   angiogenesis in prenatal human brain. *Cell*. 2022;185(20):3753-3769.e18.

423   doi:10.1016/j.cell.2022.09.004

424   27. Ihara M, Yamamoto Y. Transcriptomic mapping of the human cerebrovasculature. *Nat Rev Neurol*.

425   2022;18(6):319-320. doi:10.1038/s41582-022-00650-9

426   28. Fujioka T, Kaneko N, Sawamoto K. Blood vessels as a scaffold for neuronal migration.

427   *Neurochemistry International*. 2019;126:69-73. doi:10.1016/j.neuint.2019.03.001

428   29. Tsai HH, Niu J, Munji R, et al. Oligodendrocyte precursors migrate along vasculature in the

429   developing nervous system. *Science*. 2016;351(6271):379-384. doi:10.1126/science.aad3839

430   30. Bergles DE, Richardson WD. Oligodendrocyte Development and Plasticity. *Cold Spring Harb*

431   *Perspect Biol*. 2016;8(2):a020453. doi:10.1101/cshperspect.a020453

432   31. Barber M, Pierani A. Tangential migration of glutamatergic neurons and cortical patterning during

433   development: Lessons from Cajal-Retzius cells. *Developmental Neurobiology*. 2016;76(8):847-881.

434   doi:10.1002/dneu.22363

435   32. Elorriaga V, Pierani A, Causeret F. Cajal-retzius cells: Recent advances in identity and function.

436   *Current Opinion in Neurobiology*. 2023;79:102686. doi:10.1016/j.conb.2023.102686

437   33. Causeret F, Moreau MX, Pierani A, Blanquie O. The multiple facets of Cajal-Retzius neurons.

438   *Development*. 2021;148(11):dev199409. doi:10.1242/dev.199409

439   34. Olynik BM, Rastegar M. The Genetic and Epigenetic Journey of Embryonic Stem Cells into Mature

440   Neural Cells. *Front Gene*. 2012;3. doi:10.3389/fgene.2012.00081

441 35. Moretto E, Murru L, Martano G, Sassone J, Passafaro M. Glutamatergic synapses in

442   neurodevelopmental disorders. *Progress in Neuro-Psychopharmacology and Biological Psychiatry*.

443   2018;84:328-342. doi:10.1016/j.pnpbp.2017.09.014

444 36. Tang X, Jaenisch R, Sur M. The role of GABAergic signalling in neurodevelopmental disorders. *Nat*

445   *Rev Neurosci*. 2021;22(5):290-307. doi:10.1038/s41583-021-00443-x

446 37. Tartaglia M, Aoki Y, Gelb BD. The molecular genetics of RASOPATHIES : An update on novel

447   disease genes and new disorders. *American J of Med Genetics Pt C*. 2022;190(4):425-439.

448   doi:10.1002/ajmg.c.32012

449 38. Zenker M. Clinical overview on RASOPATHIES. *American J of Med Genetics Pt C*. 2022;190(4):414-

450   424. doi:10.1002/ajmg.c.32015

451 39. Knapp K, Naik N, Ray S, Van Haaften G, Bicknell LS. Histones: coming of age in Mendelian genetic

452   disorders. *J Med Genet*. 2023;60(3):1-10. doi:10.1136/jmg-2022-109085

453 40. Dixon-Salazar TJ, Gleeson JG. Genetic regulation of human brain development: lessons from

454   Mendelian diseases. *Annals of the New York Academy of Sciences*. 2010;1214(1):156-167.

455   doi:10.1111/j.1749-6632.2010.05819.x

456 41. Hao Y, Hao S, Andersen-Nissen E, et al. Integrated analysis of multimodal single-cell data. *Cell*.

457   2021;184(13):3573-3587.e29. doi:10.1016/j.cell.2021.04.048

458 42. Bjornsson HT. The Mendelian disorders of the epigenetic machinery. *Genome Res*.

459   2015;25(10):1473-1481. doi:10.1101/gr.190629.115

460 43. Hamilton MJ, Newbury-Ecob R, Holder-Espinasse M, et al. Rubinstein–Taybi syndrome type 2:

461   report of nine new cases that extend the phenotypic and genotypic spectrum. *Clinical*

462   *Dysmorphology*. 2016;25(4):135-145. doi:10.1097/MCD.0000000000000143

19

463   44. López M, García-Oguiza A, Armstrong J, et al. Rubinstein-Taybi 2 associated to novel EP300

464   mutations: deepening the clinical and genetic spectrum. *BMC Med Genet*. 2018;19(1):36.

465   doi:10.1186/s12881-018-0548-2

466   45. Van Gils J, Magdinier F, Fergelot P, Lacombe D. Rubinstein-Taybi Syndrome: A Model of

467   Epigenetic Disorder. *Genes*. 2021;12(7):968. doi:10.3390/genes12070968

468   46. Fergelot P, Van Belzen M, Van Gils J, et al. Phenotype and genotype in 52 patients with Rubinstein–

469   Taybi syndrome caused by *EP300* mutations. *American J of Med Genetics Pt A*. 2016;170(12):3069-

470   3082. doi:10.1002/ajmg.a.37940

471   47. Geraldo AF, Rossi A, Severino M. Malformations of Cortical Development. In: *Pediatric*

472   *Neuroradiology*. Springer, Berlin, Heidelberg; 2021.

473   48. Gelb BD, Cavé H, Dillon MW, et al. ClinGen's RASopathy Expert Panel consensus methods for

474   variant interpretation. *Genetics in Medicine*. 2018;20(11):1334-1345. doi:10.1038/gim.2018.3

475   49. Thaxton C, Goldstein J, DiStefano M, et al. Lumping versus splitting: How to approach defining a

476   disease to enable accurate genomic curation. *Cell Genomics*. 2022;2(5):100131.

477   doi:10.1016/j.xgen.2022.100131

478   50. Breen MS, Ozcan S, Ramsey JM, et al. Temporal proteomic profiling of postnatal human cortical

479   development. *Transl Psychiatry*. 2018;8(1):267. doi:10.1038/s41398-018-0306-4

480   51. R Core Team. R: A language and environment for statistical computing. Published online 2021.

481   https://www.R-project.org/

482   52. Chang W, Cheng J, Allaire J, et al. shiny: Web Application Framework for R. Published online

483   November 17, 2023. https://github.com/rstudio/shiny ; https://shiny.posit.co/

484   53. Wickham H, Chang W, Henry L, et al. ggplot2: Elegant Graphics for Data Analysis. Published online

485   2016. https://ggplot2.tidyverse.org

486

487

488   **Figure Legends**

489   **Figure 1 NeuroTri2-VISDOT fills key gap to inform selection of Mendelian NDD models.** A)

490   Proposed systematic approach to go from identification of putative Mendelian NDD gene to cohort

491   identification to selection of the most useful model for downstream mechanistic work. Black box

492   represents the gap filled by NeuroTri2-VISDOT. B) Timeline of human prenatal neurodevelopment

493   including first- (gestational weeks (GW) 1-13; light gray), second- (GW 14-27; gold), and third-trimester

494   (GW 28-40; gray), as well as the beginning of postnatal neurodevelopment (charcoal). All boxes/lines that

495   extend past GW40 indicate continuance into postnatal life. Unfilled gold box highlights the second

496   trimester of neurodevelopment, including the cell types present and the ongoing neurodevelopmental

497   processes.

498

499   **Table 1 Primer on transcriptomically-delineated cell types in Bhaduri et al dataset.**

500

501   **Figure 2 NeuroTri2-VISDOT captures genotypic and phenotypic heterogeneity of established**

502   **NDDs.** (A,C-D) Dot plots (left) – the average expression scaled reflects the normalized expression value

503   for a gene, scaled to zero, and depicted by color gradient; the percent expression reflects the percentage of

504   a particular cell type with at least one read mapping to the gene of interest, depicted by size gradient. Line

505   plots (right) – percent expression by cell type. A) Dot plots (left) and percent expression line plots (right)

506   for *CREBBP* and *EP300* across 10 neural cell types and 8 second-trimester time points. Unfilled boxes

507   highlight GW18, emphasized in text. B) Table of genes associated with NS (left) and NS-like

508   RASopathies (right). C) Dot plots (left) and percent expression line plots (right) for NS genes. Unfilled

509   boxes highlight GW18, emphasized in text. D) Dot plots (left) and percent expression line plots (right) for

510   NS-like RASopathy genes. Unfilled arrows highlight plots for the recently identified RASopathy genes,

511   *CDC42* and *YWHAZ.* Gray arrows highlight plots for *SHOC* and *PPP1CB*, the genes underlying NSLAH.

512   Black arrows highlight plots for *HRAS, KRAS* and *MAP2K2.*

513   Abbreviations: NDDs = neurodevelopmental disorders; NS = Noonan Syndrome; NSML = NS with

514   multiple lentigines; NSLAH = NS-like disorder with loose anagen hair; CFCS = Cardiofaciocutaneous

515   Syndrome; CS = Costello Syndrome; GW = gestational week.

516

517   **Figure 3 Novel application of NeuroTri2-VISDOT to histone-associated NDDs.** A) Table of RI

518   histone genes delineating which are known or predicted to be associated with NDDs. (B-D) Dot plots

519   (left) – the average expression scaled reflects the normalized expression value for a gene, scaled to zero,

520   and depicted by color gradient; the percent expression reflects the percentage of a particular cell type with

521   at least one read mapping to the gene of interest, depicted by size gradient. Line plots (right) – percent

522   expression by cell type. Unfilled boxes highlight GW16, emphasized in text. B) Dot plots (left) and

523   percent expression line plots (right) for RI histone genes with known Mendelian NDD association. C) Dot

524   plots (left) and percent expression plots (right) for RI histone genes with predicted Mendelian NDD

525   association. D) Dot plots (left) and percent expression plots (right) for RI histone genes without known or

526   predicted Mendelian NDD association.

527   Abbreviations: NDDs = neurodevelopmental disorders; RI = replication-independent; GW = gestational

528   week.

529

530   **Figure 4 Uses and future applications of NeuroTri2-VISDOT.** NeuroTri2-VISDOT can be used, as

531   demonstrated, at the level of a translational genetic research lab to inform model selection. More broadly,

532   similar tools can be built to address the same questions in other tissues and at other developmental stages

533   using different data sets. Expression signatures can also be compared across multiple genes in BioBanks

534   to nominate candidate causative genes.

535

Data Availability

Data and code used to generate NeuroTri2-VISDOT can be found at https://github.com/kellyclark1/VISDOT.

Acknowledgements

Funding Statement

Author Contributions

CRediT has 14 categories:
1. Conceptualization – KJC, EEL, EMG, TTN, EBJ
2. Data curation – EEL, KJC, EMG
3. Formal analysis – KJC, EEL, EMG
4. Funding acquisition – RAN, EJB
5. Investigation – KJC, EEL, EMG
6. Methodology – KJC, EEL, EMG, TTN, EJB
7. Project administration – TTN, EJB
8. Resources – RAN, EJB
9. Software - KJC
10. Supervision – TTN, EJB
11. Validation – KJC, EEL, EMG, AKS, DLC, ELD, RAN, TTN, EJB
12. Visualization – KJC, EEL
13. Writing-original draft – EEL, KJC
14. Writing-review & editing – EEL, KJC, EMG, AKS, DLC, ELD, RAN, TTN, EJB

Ethics Declaration

This study does not involve human subjects or live invertebrate and/or higher invertebrates.

Conflict of Interest

The authors declare no conflicts of interest.
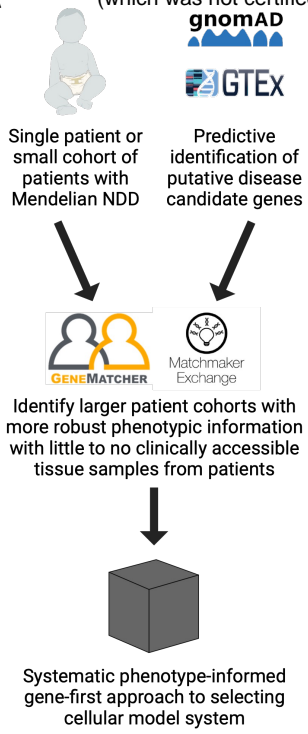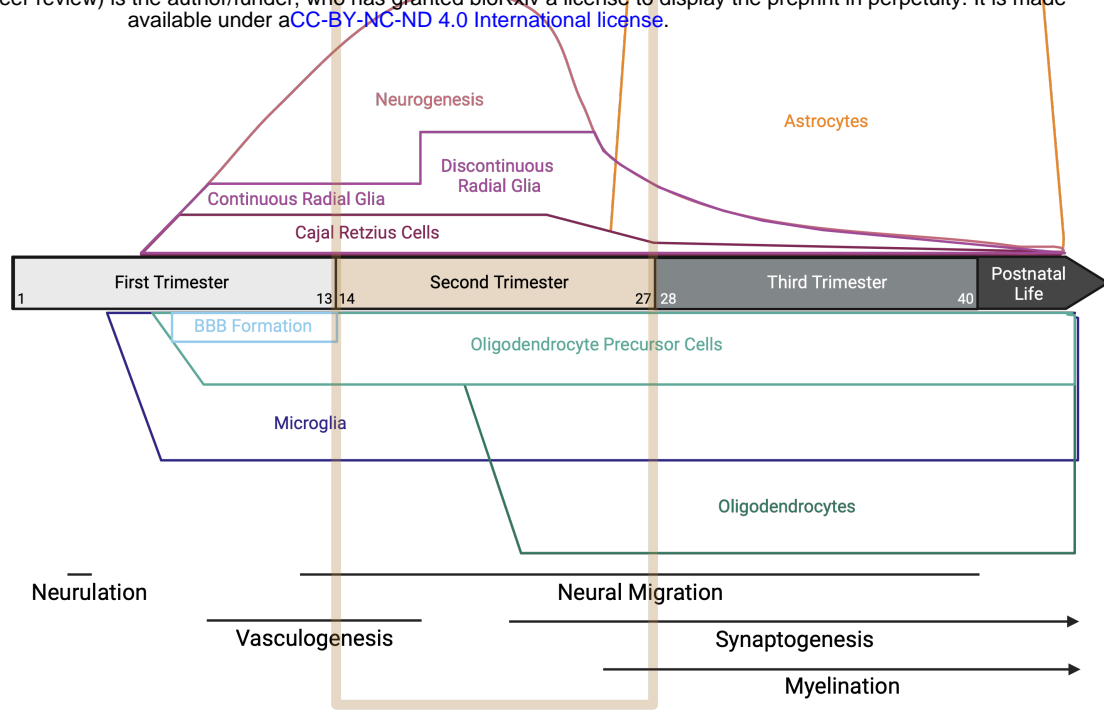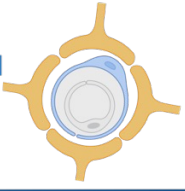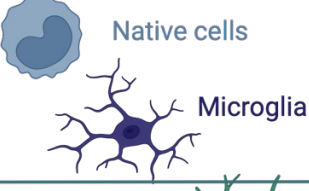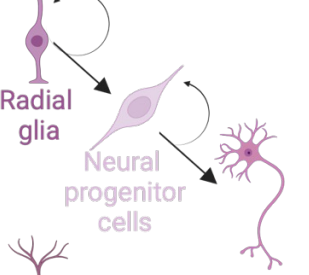
Figure 1 NeuroTri2-VISDOT fills key gap to inform selection of Mendelian NDD models.

Table 1 Primer on transcriptomically-delineated cell types in the Bhaduri et al dataset

			Origin	Function	Refs
Endothelial Cells[1]	Endothelial cells		Mesodermally-derived, modified squamous epithelial cells	• Form the walls of the blood vessels that regulate the interactions with different vascular, immune and neural cells as well as the movement of ions, nutrients, hormones, gases, metabolites, drugs and cells into the brain • One of the two key cell types (in addition to mural cells) that constitute the main structural and functional vascular elements • Vascular maturation and angiogenesis play critical roles in human neurodevelopment, including in vascular-guided migration of GABAergic interneurons	24, 25, 26, 27, 28
Immune Cells[1]	Native cells / Microglia		Myeloid cells derived from embryonic hematopoietic progenitors of the yolk sac and fetal liver	• Colonize the brain parenchyma beginning in GW4 • Play an increasingly recognized role in neurodevelopment, and a potentially pathophysiologic role in the pathogenesis of Mendelian and multi-gene neurodegenerative disorders • **Native cells:** non-parenchymal macrophages including perivascular, choroid plexus and meningeal macrophages • **Microglia:** predominant immune cells of the brain that serve as tissue-resident macrophages	16, 17, 18, 19
Glia[1]	Oligodendrocyte precursor cells		Originate from the ventral ventricular zone of the medial and lateral GEs	• Migrate along the vasculature from the medial and lateral GEs • Only glial cells that form direct synapses with neurons • Differentiate into oligodendrocytes, which myelinate neuronal axons in the central nervous system	29, 30
Neuronal Populations[1]	Cajal-Retzius cells		Extraneocortically derived	• Pioneer neurons of the human cerebral cortex that are required for cortical layering through the secretion of reelin; the radial migration of glutamatergic neurons, GABAergic neurons and OPCs; functional area formation; as well as dendritogenesis and synaptogenesis • Largely transient population that apoptose in humans between GW23-28	31, 32, 33

	Radial glia / Neural progenitor cells / Glutamatergic neurons		Neuroepithelially-derived	• **Radial glia:** stem cells of the subventricular zone that begin to divide asymmetrically at GW 7 until, in a human-specific process, they become a physically discontinuous scaffold during GW 16-17
				  ○ Contribute to the formation of glutamatergic neurons and also provide a physical scaffold for their radial migration
				  ○ After the peak of neurogenesis, radial glia differentiate into astrocytes
				• Asymmetric division of outer radial glia generate **neural progenitor cells** which then differentiate into **glutamatergic neurons** of the cerebral cortex
				  ○ **Neural progenitor cells** are an intermediary precursor population between radial glia and more differentiated neurons
				  ○ **Glutamatergic neurons** are a class of excitatory neurons that release glutamate and play essential roles in synaptic transmission, plasticity, and long-term potentiation
					21, 22, 34, 35

	GABAergic interneurons		Derived from progenitors within the ventricular-subventricular zones and GEs	• Inhibitory interneurons that migrate tangentially towards the cortex along blood vessels • Shape the connectivity of neural networks; regulate the excitability of circuits; and modulate the activity and plasticity of the brain	19, 28, 31, 36

[1] The color-coding aligns with the colors of the prenatal to early postnatal human neurodevelopment timeline from Figure 1B
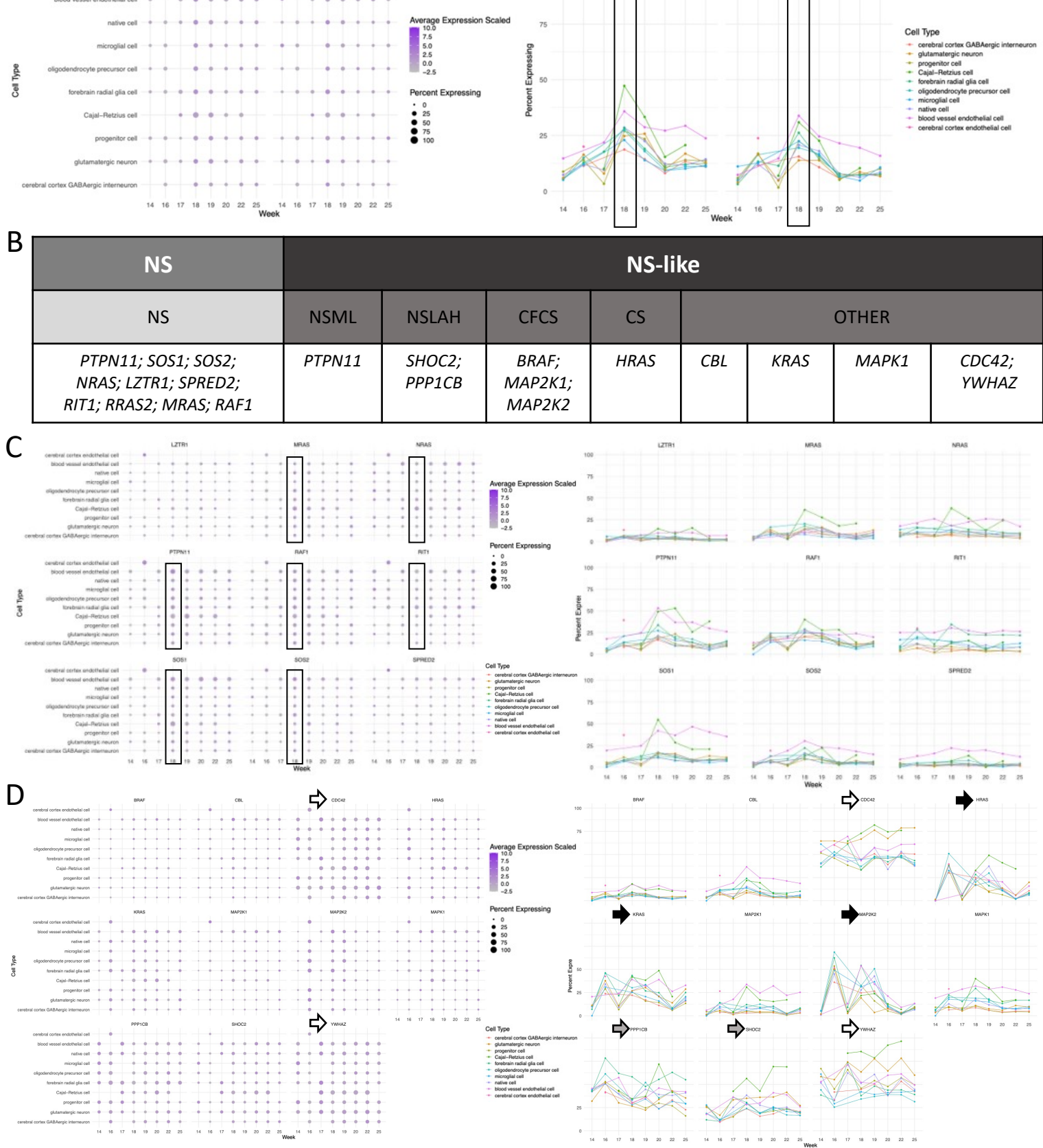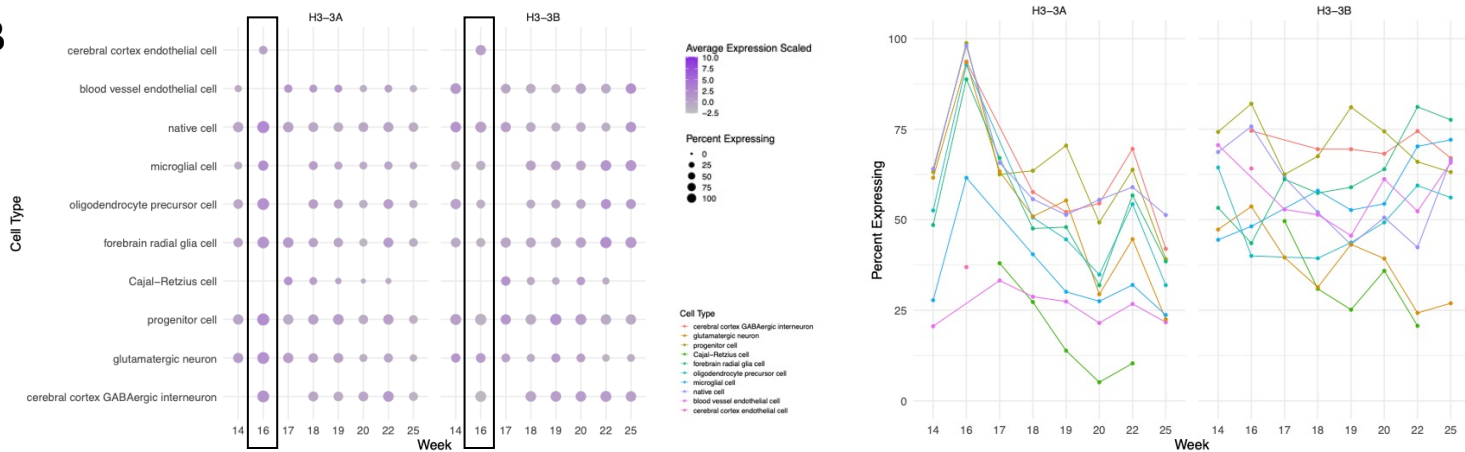
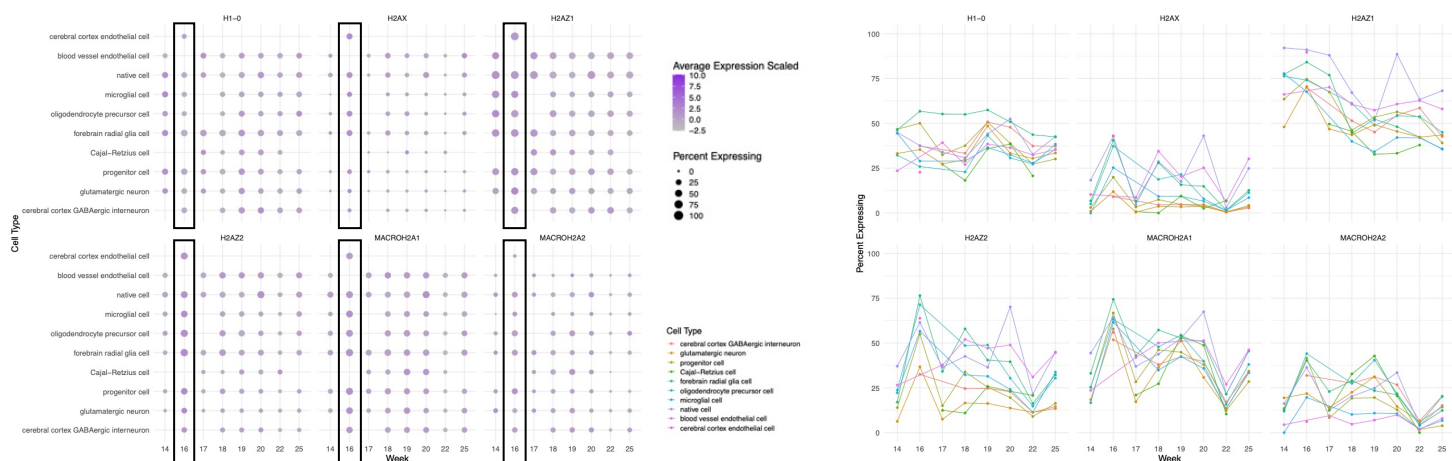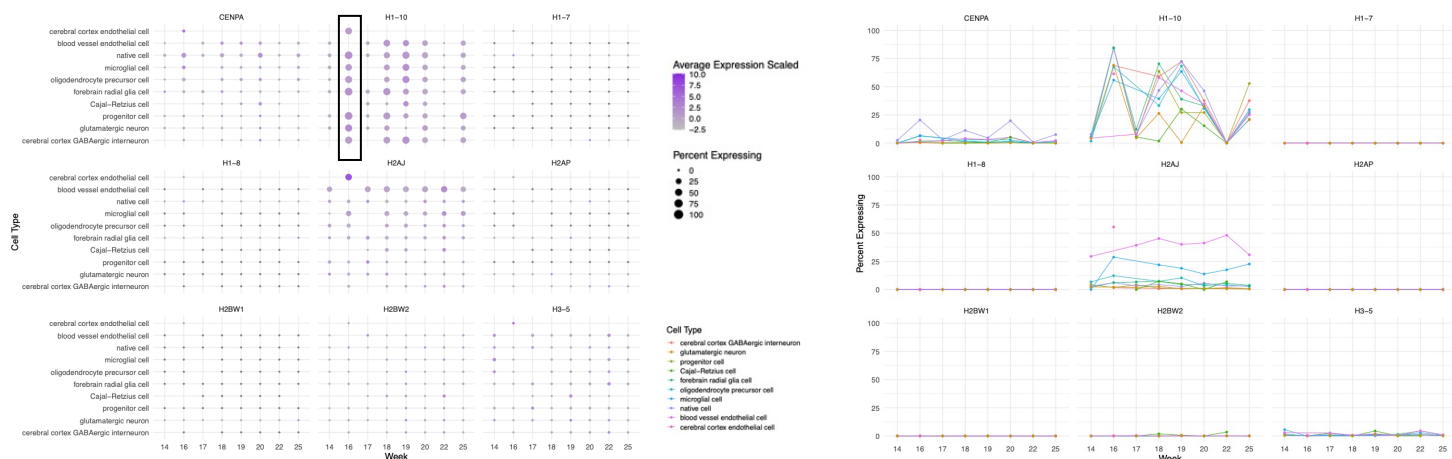**Figure 2 NeuroTri2-VISDOT captures genotypic and phenotypic heterogeneity of established NDDs.**

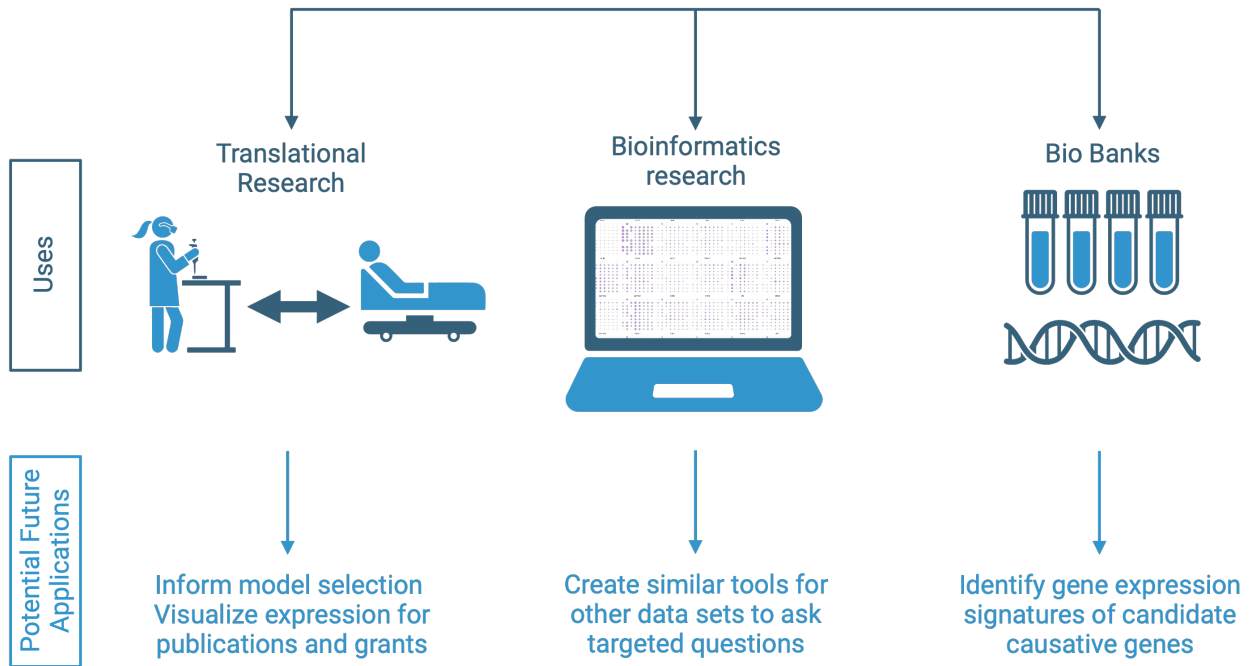**Figure 3 Novel application of NeuroTri2-VISDOT to histone-associated NDDs.**

Figure 4 Uses and future applications of NeuroTri2-VISDOT.